

Supporting Information

The insight into the mechanism of carboxylic acids hydrogenation into alcohols at MnO/Cu interface: A combined DFT and kinetic Study

Jingbo Du^{a,b,c}, , Yifei Chen^{a,b,c}, Lingtao Wang^{a,b,c}, Minhua Zhang^{a,b,c*}

^aKey Laboratory for Green Chemical Technology of Ministry of Education, R&D Center for Petrochemical Technology, Tianjin University, Tianjin 300072, China

^bZhejiang Institute of Tianjin University, Ningbo, Zhejiang, 315201, China

^cState Key Laboratory of Engines, Tianjin University, Tianjin 300072, China

*Corresponding author. Tel.: +86-22-27406119; fax: +86-22-27406119. E-mail address: mhzhang@tju.edu.cn.

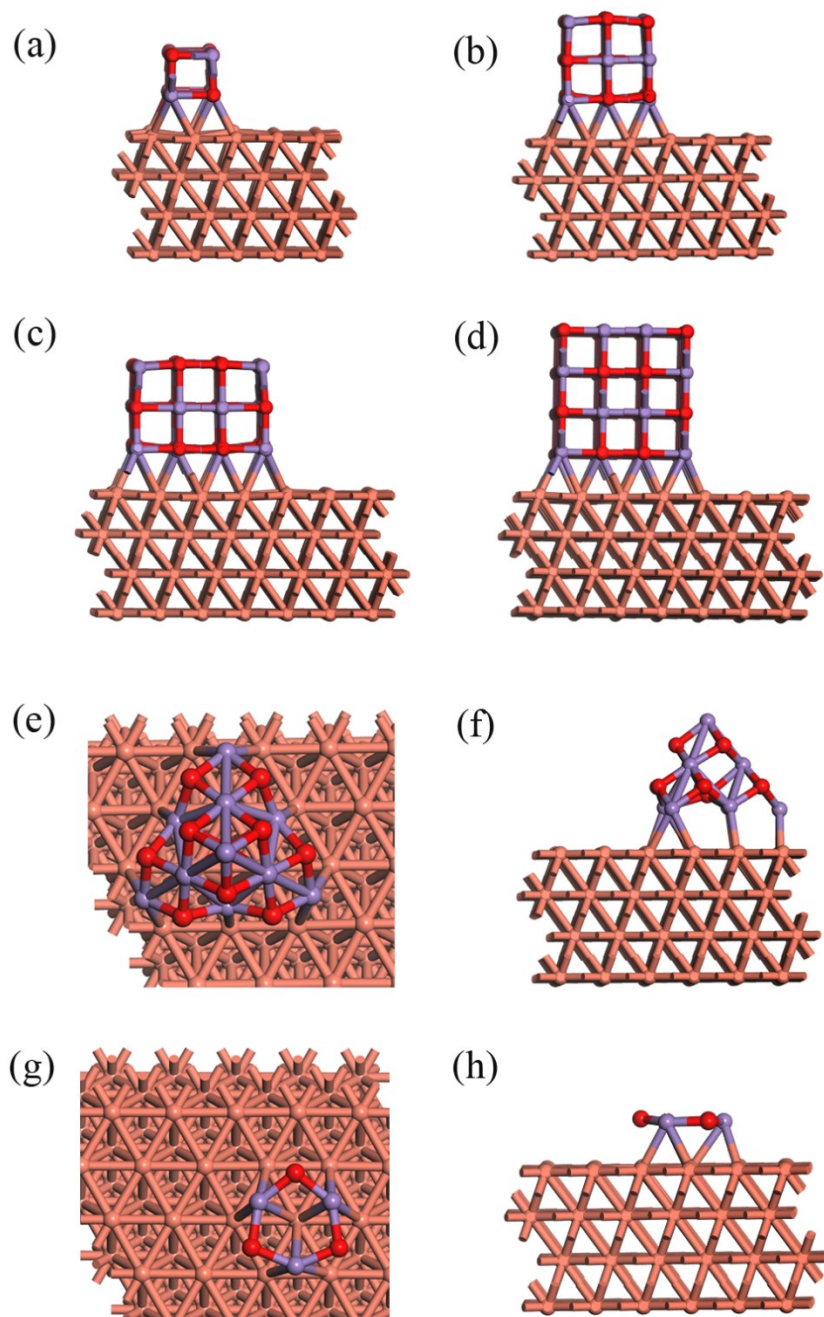


Fig. S1. The MnO/Cu (111) model candidates for the HDO process of acetic acid to ethanol. (a) $\text{MnO}_{2*2}/\text{Cu}$ (111) model. (b) $\text{MnO}_{3*3}/\text{Cu}$ (111) model (used in the main text). (c) $\text{MnO}_{4*3}/\text{Cu}$ (111) model. (d) $\text{MnO}_{4*4}/\text{Cu}$ (111) model. (e, f) Top view and side view of $\text{MnO}_{10\text{-clu}}/\text{Cu}$ (111) model (g, h) Top view and side view of $\text{MnO}_{3\text{-clu}}/\text{Cu}$ (111) model.

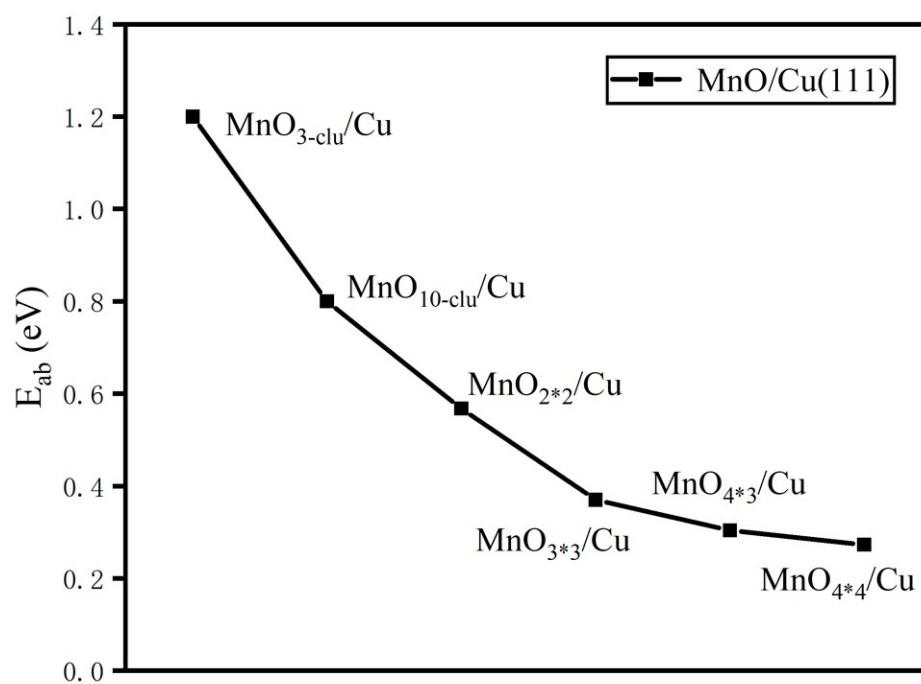


Fig. S2. The coverage binding energies (E_{ab}) of different MnO/Cu (111) model. The names of the model inside the picture correspond to that in Fig. S1.

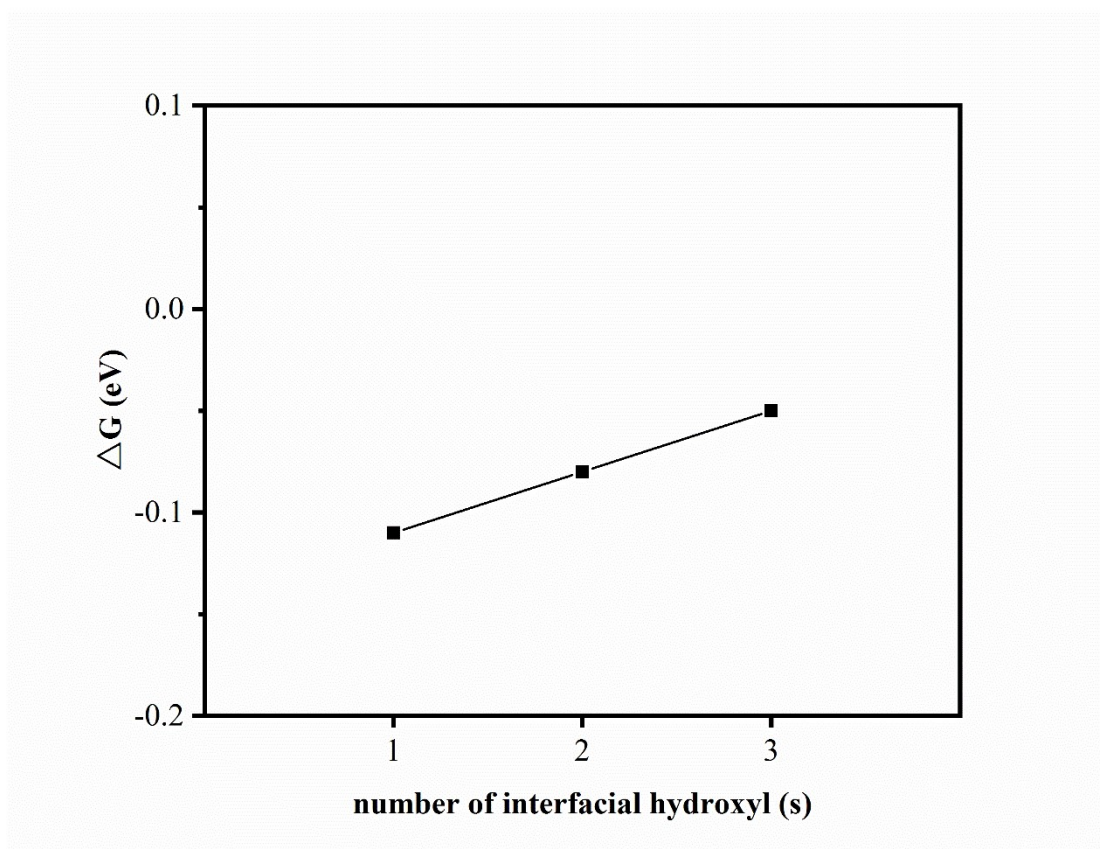


Fig. S3. Gibbs free energy change during the generation of with different number of interfacial hydroxyls.

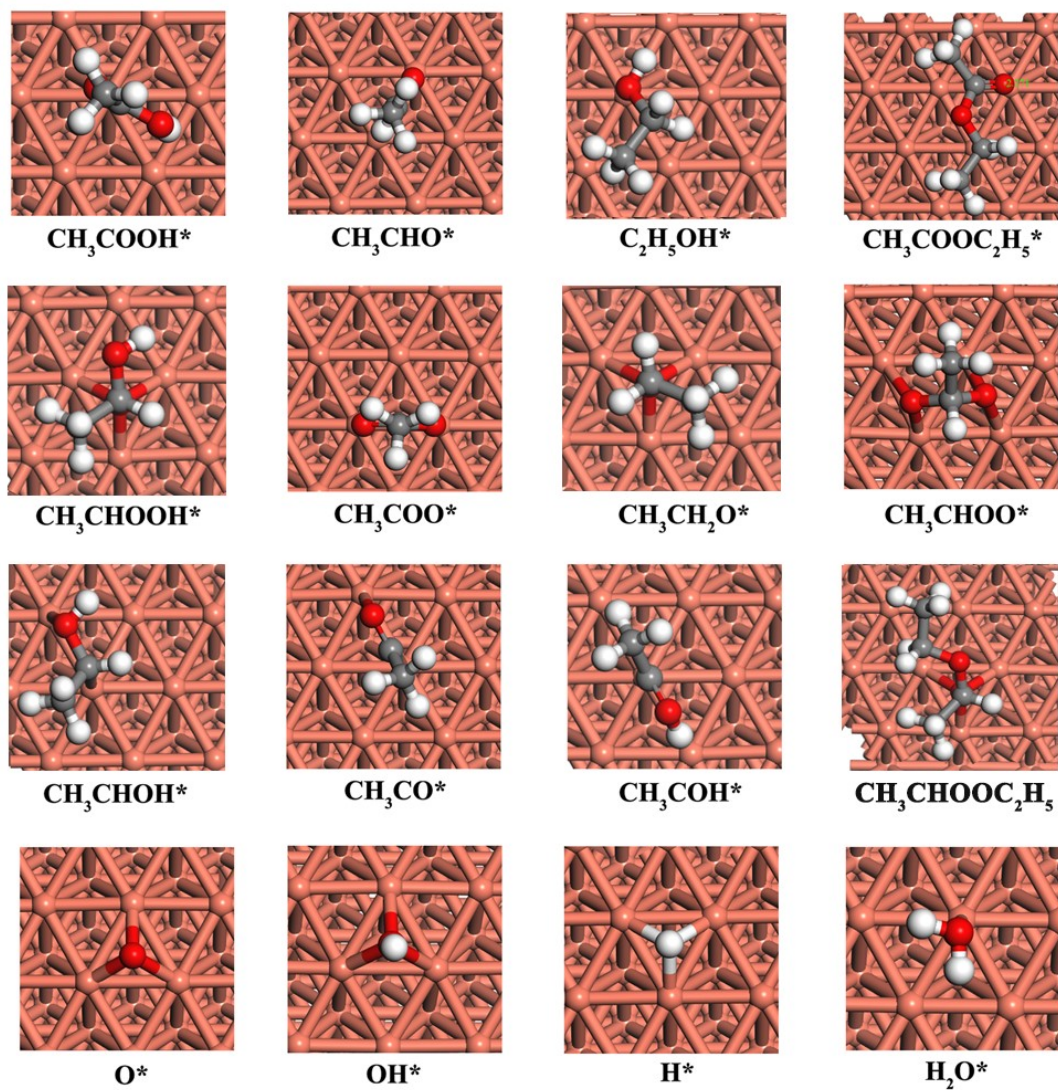
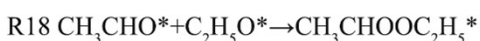
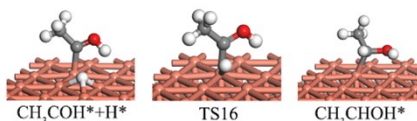
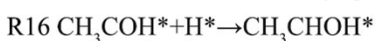
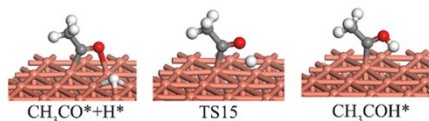
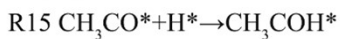
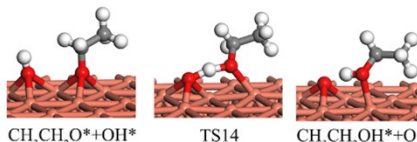
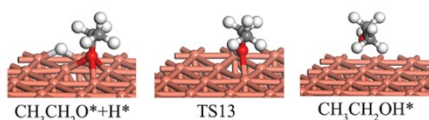
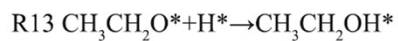
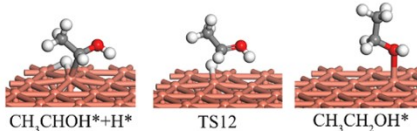
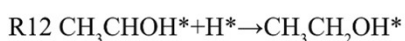
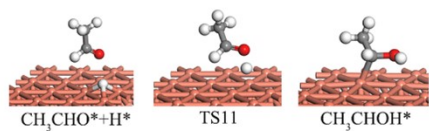
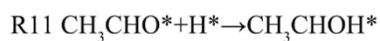
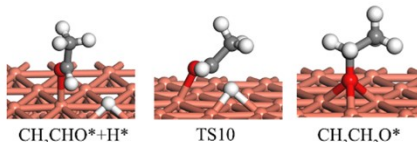
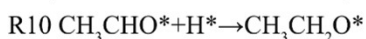
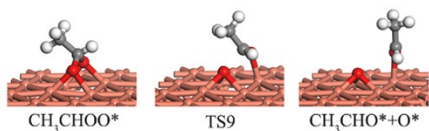
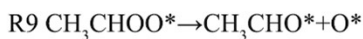
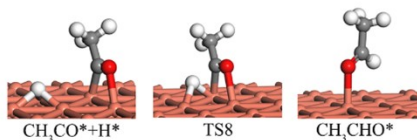
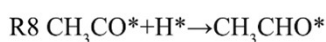
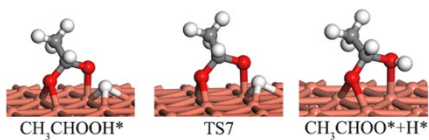
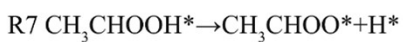
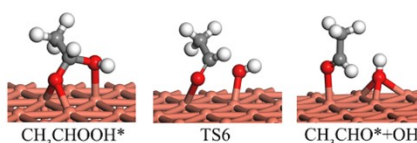
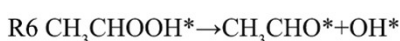
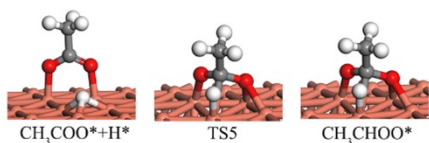
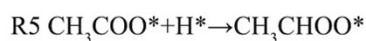
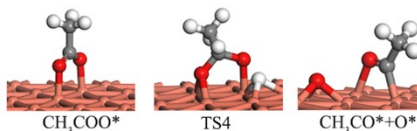
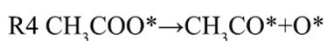
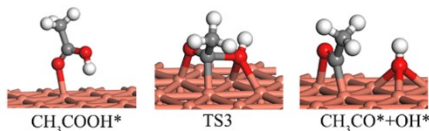
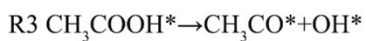
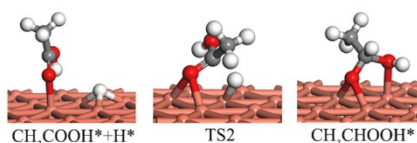
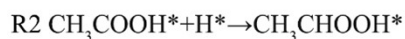
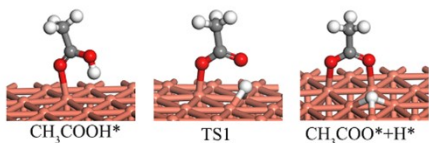
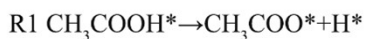


Fig. S4. The configuration of adsorbates involved in the HDO process of acetic acid on the Cu (111) surface



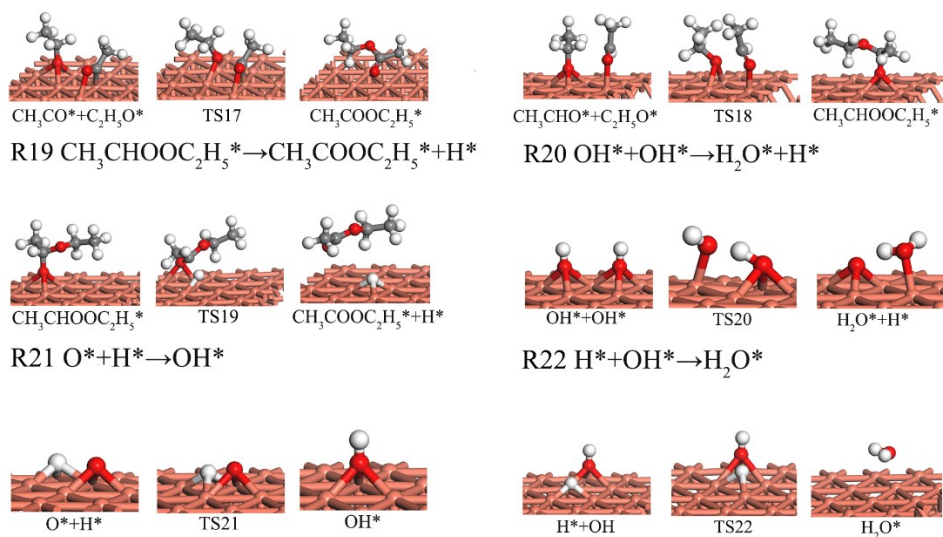


Fig. S5. The configuration of IS, TS and FS of the each elementary step involved in the conversion of acetic acid on the Cu (111) surface

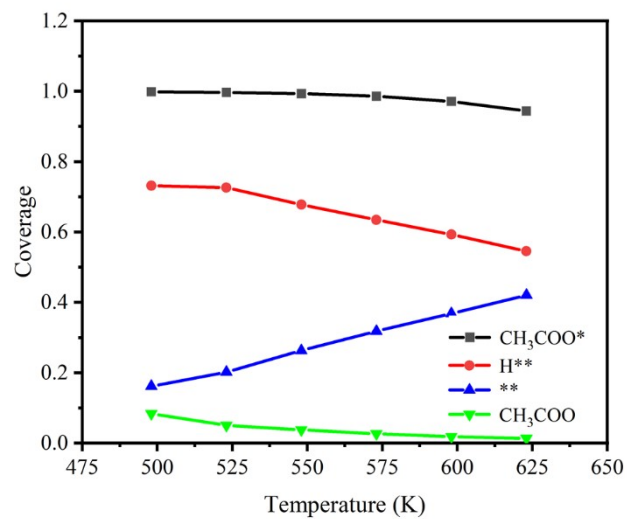


Fig. S6. The coverage of main surface species at interfacial (*) and Cu sites (**) as a function of temperature.

SI-1 Method and Validation to obtain the optimal MnO/Cu (111) interface model

As mentioned in the Section 2, the Cu (111) surface and the MnO (100)-like stripe was chosen to build the MnO/Cu (111) model. In view of various possible configurations, the scanning method was applied here to gain the optimal structure. The MnO stripe was manually put parallel to the Cu (111) surface along the lattice-parameter-matched direction (y axis in the current paper) as the initial candidate. Then the MnO stripe translated along the x, y and z axis to produce new candidates. The rotation of the MnO stripe would lead to the increased mismatch of lattice parameter between the upper MnO and lower copper atoms which was forbidden in the initial guesses. Then the generated possible configurations were allowed to relaxed until the force was less than 0.02eV/Å. The interval was set to 0.02, 0.03 and 0.025 (in direct coordinates) during the generation of new configurations along the x, y and z axis, respectively. Then the structure with the lowest total energies was chosen for the following investigations.

There were various MnO structures which could be used to construct the MnO/Cu interface model. Actually, the MnO cluster was the first choice to simulation the MnO/Cu interface during the modelling process because the interfacial Mn atoms had lower coordinate numbers (i.e., higher degree of unsaturation) which maybe led to better activities. However, the stability of Mn-Cu interface was also an important factor which determine the catalytic performance over a long period of time because the Cu-based catalyst usually suffered from the sintering problem. The average binding energies (E_{ab}) was employed here to evaluate the stability of MnO/Cu interface which was calculated by the following equation:

$$E_{ab} = \frac{E_{MnO/Cu(111)} - E_{Cu(111)} - N \cdot E_{MnO}}{N}$$

Where $E_{MnO/Cu(111)}$, $E_{Cu(111)}$ and E_{MnO} represented the energies of the total MnO/Cu (111) model, the substrate Cu(111) model and the every MnO unit in the MnO bulk, respectively. In addition, the N was the number of MnO unit used for the MnO/Cu (111) surface. The E_{ab} indeed referred to the energy (stability) difference between the interfacial MnO cluster and the MnO bulk. Because the MnO unit was usually more stable in the bulk, the E_{ab} was more than 0. The smaller value expressed that the interfacial MnO moiety had better resistance to agglomeration. According to the previously reported metal/oxide interface, we constructed MnO-cluster/Cu (111) model with different sizes which were consisted of 3MnO units (MnO_{3-clu}/Cu (111) surface) and 10 MnO units (MnO_{10-clu}/Cu (111) surface), respectively. In addition, the ribbons with different atomic layers of MnO were also adopted to compare with the MnO-clu/Cu (111) model. The MnO_{x*y}/Cu (111) meant that the width and thickness of MnO ribbon used for interface were x and y atomic layers, respectively. The configurations of relevant MnO-clu/Cu (111) and MnO_{x*y}/Cu (111) were summarized in Fig. S1.

As shown in Fig. S2., the E_{ab} became lower with the addition of more MnO units. Compared with the MnO-cluster/Cu (111) model, the MnO_{x*y}/Cu (111) model exhibited much lower E_{ab} when using the MnO ribbon not less than (3x3), meaning that the currently employed MnO/Cu (111) interfacial model had better stability for the following HDO process of acetic acid. As a result, we adopt the MnO ribbon instead of MnO cluster to build the MnO/Cu (111) model.

For the second question that “Does three atomic layers of MnO enough to model the

Cu-MnO interface”, we checked the energies change between $\text{MnO}_{3*3}/\text{Cu}$ (111) and larger $\text{MnO}_{4*4}/\text{Cu}$ (111) model. The result showed that the barrier of rate-limiting step (RDS, R2) and relevant adsorption energies of key intermediate such as CH_3COOH^* and $\text{CH}_3\text{CHOOH}^*$ were almost unchanged at the $\text{MnO}_{4*4}/\text{Cu}$ (111) model (less than 0.02 eV), meaning that the currently used $\text{MnO}_{3*3}/\text{Cu}$ (111) model would be capable of obtaining accurate energies in the HDO process. As a result, we think that the (3x3) MnO ribbon was enough to represent the MnO/Cu (111) interface.

Table S1 Coverage of each species in the conversion of acetic acid at the MnO/Cu (111) surface.

The *, ** and *** represented the interfacial Mn site, Cu site and interfacial O site, respectively.

Species	Coverage	Species	Coverage
θ_{RCOOH^*}	1.10E-05	$\theta_{\text{RCOOH}^{**}}$	4.12e-05
θ_{RCOO^*}	9.88E-03	$\theta_{\text{RCHOH}^{**}}$	2.37e-10
θ_{RCHOOH^*}	1.55E-09	$\theta_{\text{RCO}^{**}}$	1.03e-10
θ_{RCO^*}	5.50E-12	$\theta_{\text{OH}^{**}}$	1.48e-06
θ_{OH^*}	1.57e-08	$\theta_{\text{RCH}_2\text{O}^{**}}$	1.56e-05
θ_{O^*}	3.96e-07	$\theta_{\text{RCHOOC}_2\text{H}_5^{**}}$	3.45e-13
θ_{RCHOO^*}	7.89e-12	$\theta_{\text{RCHO}^{**}}$	3.04e-09
$\theta_{\text{RCH}_2\text{O}^*}$	2.02e-07	$\theta_{\text{RCH}_2\text{OH}^{**}}$	4.01e-06
θ_{RCHOH^*}	2.24e-14	$\theta_{\text{RCOOC}_2\text{H}_5^{**}}$	1.65e-16
θ_{RCOH^*}	3.77e-18	$\theta_{\text{H}_2\text{O}^{**}}$	8.24e-04
$\theta_{\text{RCHOOC}_2\text{H}_5^*}$	2.19e-11	$\theta_{\text{H}^{**}}$	8.49e-01
θ_{RCHO^*}	1.82E-09	θ_{**}	1.29e-01
$\theta_{\text{RCH}_2\text{OH}^*}$	2.41E-06	$\theta_{\text{H}^{***}}$	9.08e-03
$\theta_{\text{RCOOC}_2\text{H}_5^*}$	1.12E-15	θ_{***}	9.24e-04
$\theta_{\text{H}_2\text{O}^*}$	6.33E-07		
θ_*	9.94E-05		

Table S2 Coverage of each species in the conversion of acetic acid on the Cu (111) surface.

Species	Coverage
θ_{RCOOH^*}	7.48E-05
θ_{RCOO^*}	2.44E-02
θ_{RCHOOH^*}	4.05E-10
θ_{RCO^*}	1.63E-11
θ_{OH^*}	1.64E-06
θ_{O^*}	3.52E-10
θ_{RCHOO^*}	3.29E-13
$\theta_{\text{RCH}_2\text{O}^*}$	5.67E-06
θ_{RCHOH^*}	1.49E-14
θ_{RCOH^*}	5.19E-15
$\theta_{\text{RCHOOC}_2\text{H}_5^*}$	1.19E-13
θ_{RCHO^*}	2.71E-09
$\theta_{\text{RCH}_2\text{OH}^*}$	2.17E-06
$\theta_{\text{RCOOC}_2\text{H}_5^*}$	6.73E-15
$\theta_{\text{H}_2\text{O}^*}$	1.59E-06
θ_{H^*}	6.88E-01
$\theta_{\text{*}}$	2.87E-01

TableS3. The barrier along the forward and backward directions in Gibbs free energy and corresponding rates of every elementary reaction involved in the HDO process of acetic acid on Cu (111) surface. The X* represented the adsorbed on the Cu site.

Elementary Reaction	Ga (eV)	G-a (eV)	Rates (s-1)
R1: RCOOH* + * - RCOO* + H*	0.47	0.80	1.82E-03
R2: RCOOH* + H* - RCHOOH* + *	1.07	0.50	1.34E-01
R3: RCOOH* + * - RCO* + OH*	1.46	0.65	4.09E-05
R4: RCOO* + * - RCO* + O*	1.96	0.30	5.53E-07
R5: RCOO* + H* - RCHOO* + *	1.60	0.48	1.82E-03
R6: RCHOOH* + * - RCHO* + OH*	0.38	0.32	1.34E-01
R7: RCHOOH* + * - RCHOO* + H*	1.10	0.80	5.39E-08
R8: RCO* + H* - RCHO* + *	0.50	0.72	4.10E-05
R9: RCHOO* + * - RCHO* + O*	0.38	0.19	1.82E-03
R10: RCHO* + H* - RCH ₂ O* + *	0.53	0.89	1.29E-01
R11: RCHO* + H* - RCHOH* + *	0.84	0.23	2.34E-03
R12: RCHOH* + H* - RCH ₂ OH* + *	0.09	0.98	2.34E-03
R13: RCH ₂ O* + H* - RCH ₂ OH* + *	1.01	0.85	1.31E-01
R14: RCH ₂ O* + OH* - RCH ₂ OH* + O*	0.64	0.39	-2.22E-03
R15: RCO* + H* - RCOH* + *	0.81	0.37	4.43E-07
R16: RCOH* + H* - RCHOH* + *	0.54	0.59	4.43E-07
R17: RCO* + RCH ₂ O* - RCOOC ₂ H ₅ * + *	0.67	1.36	1.45E-09
R18: RCHO (g) + RCH ₂ O* - RCHOOC ₂ H ₅ *	0.48	0.52	8.45E-06
R19: RCHOOC ₂ H ₅ * + * - RCOOC ₂ H ₅ * + H*	0.59	0.94	8.45E-06
R20: 2OH* - H ₂ O* + O*	0.32	0.13	4.23E-04
R21: O* + H* - OH* + *	0.91	1.43	2.89E-05
R22: OH* + H* - H ₂ O* + *	1.02	0.99	1.35E-01
R23: RCOOH (g) + * - RCOOH*	0.41	0.00	1.36E-01
R24: H ₂ (g) + 2* - 2H*	0.80	0.73	2.67E-01
R25: RCHO* - RCHO(g) + *	0.00	0.70	4.51E-03
R26: RCH ₂ OH* - RCH ₂ OH (g) + *	0.00	0.50	1.31E-01
R27: RCOOC ₂ H ₅ * - RCOOC ₂ H ₅ (g) + *	0.00	0.80	8.46E-06
R28: H ₂ O* - H ₂ O (g) + *	0.00	0.48	1.35E-01

SI-2 Computational details involved in the kinetic simulation for the conversion of acetic acid on the MnO/Cu (111) and Cu (111) surface

To corroborate the conclusion from DFT results and gain more quantitative activities of HDO process of acetic acid, the micro-kinetic analysis was used in this paper. The rate equation of every elementary step was summarized in TableXX. Simply, the rate constant $k_i(k-i)$ of the step i was calculated based on the transition state theory (TST):

$$k = \frac{k_b T}{h} e^{-\frac{\Delta G}{k_b T}}$$

where the h , k_b and T was the Planck constant, Boltzmann constant and chosen temperature. The ΔG was the standard molar gibbs free energy change between the IS (FS) and TS. The gibbs free energies of all gaseous species (CH_3COOH , CH_3CHO , $\text{C}_2\text{H}_5\text{OH}$, $\text{CH}_3\text{COOC}_2\text{H}_5$, H_2 and H_2O) was obtained by:

$$G(T, p) = E_{\text{tot}} + \text{ZPE} + \Delta G(0 \rightarrow T, p) = E_{\text{tot}} + \text{ZPE} + \Delta G(0 \rightarrow T, P_0) - RT \ln(P/P_0)$$

where the E_{tot} , ZPE , $\Delta G(0 \rightarrow T, P_0)$ represented the DFT energies, zero point energies, the free energies change from the 0K and standard to the current temperature T and partial pressure P . Both of the ZPE and $\Delta G(0 \rightarrow T, p)$ could be obtained based on frequency calculation and the details could be found in VASPKIT code. In addition, the gibbs free energies of adsorbates was calculated by:

$$G(T) = E_{\text{tot}} + \text{ZPE} + \Delta G(0 \rightarrow T)$$

where the E_{tot} , ZPE , $\Delta G(0 \rightarrow T)$ represented the DFT energies, zero point energies, the thermal correction. The ZPE and required thermal correction could be obtained with the help of the vibrational frequency. As shown in the following two equations,

$$\text{ZPE} = \sum_i \left(\frac{v_i h}{2} \right)$$

$$\Delta G_i(0 \rightarrow T) = \sum_i \left(-k_b T \ln \frac{1}{1 - \exp\left(-\frac{v_i h}{k_b T}\right)} \right)$$

where the v_i , h , k_b and T was the frequency, Planck constant, Boltzmann constant and temperature.

The reaction conditions was set as $T=573\text{K}$, $p=2.5\text{ MPa}$, $\text{H}_2/\text{CH}_3\text{COOH} = 20$ and the conversion of acetic acid was set to be 40% which was in accordance with the previous experimental studies. The

conversion of acetic acid was assumed to obey L-H mechanism where the total reaction network was consisted of the adsorption of reactant, the generation and desorption of the products. For the adsorption of the gaseous A species, the corresponding rates was calculated by:

$$r_A = k_A \theta_* P_A / P^0 - k_{-A} \theta_{A^*}$$

where k_A and k_{-A} was the forward and backward rates constant of the elementary step $A(g) + * \rightarrow A^*$ while the P_A , θ_{A^*} and θ_* represented the partial pressure of gaseous A species, the coverage of the A species and empty site. The desorption could be seen as the reverse process of the adsorption.

For the surface reaction $B^* + C^* \rightarrow D^* + *$, the rates was obtained by:

$$r_{BC} = k_+ \theta_{B^*} \theta_{C^*} - k_- \theta_{D^*} \theta_*$$

where k_+ , k_- , θ_{B^*} , θ_{C^*} , θ_{D^*} was the forward and backward rates constant of the elementary step and the coverage of the B, C and D adsorbates on the surface. In addition, the steady-state approximation was applied here to treat the micro-kinetic model where the coverage of every kind of adsorbates was assumed unchanged ($dX/dt \approx 0$, $X = \text{adsorbates}$) in the steady state, leading to a set of closure equations. Taking the conversion of acetic acid on the Cu (111) surface as an example, the required energies was given in the TableS3 and the steady-state equations was shown in the TableS4.

TableS4 the steady-state equations of the each species X involved in the HDO process
of acetic acid on the Cu(111) surface

X species : $dX/dt = 0$

X = RCOOH*: $r_1 + r_2 + r_3 - r_{23} = 0$

X = RCOO*: $r_1 - r_4 - r_5 = 0$

X = RCHOOH*: $r_2 - r_6 - r_7 = 0$

X = RCO*: $r_3 + r_4 - r_{15} - r_8 - r_{17} = 0$

X = OH*: $r_3 + r_6 + r_{21} - 2^*r_{20} - r_{22} - r_{14} = 0$

X = O*: $r_4 + r_9 + r_{14} + r_{20} - r_{21} = 0$

X = RCHOO*: $r_5 + r_7 - r_9 = 0$

X = RCH₂O*: $r_{10} - r_{13} - r_{14} - r_{17} - r_{18} = 0$

X = RCHOH*: $r_{11} - r_{12} + r_{16} = 0$

X = RCOH*: $r_{15} - r_{16} = 0$

X = RCHOOCC₂H₅*: $r_{18} - r_{19} = 0$

X = RCHO*: $r_6 + r_8 + r_9 - r_{10} - r_{11} - r_{18} = 0$

X = RCH₂OH*: $r_{12} + r_{13} + r_{14} = 0$

X = RCOOC₂H₅*: $r_{17} + r_{19} = 0$

X = H₂O*: $r_{20} + r_{22} = 0$

X = H***: $r_1 - r_2 - r_5 + r_7 - r_8 - r_{10} - r_{11} - r_{12} - r_{13} - r_{15} - r_{16} + r_{19} - r_{21} - r_{22} + 2^*r_{24} = 0$

Note that the coverage of every adsorbate should meet the normalization condition as shown by:

$$\theta_{\text{RCOOH}^*} + \theta_{\text{RCOO}^*} + \theta_{\text{RCHOOH}^*} + \theta_{\text{RCO}^*} + \theta_{\text{OH}^*} + \theta_{\text{O}^*} + \theta_{\text{RCHOO}^*} + \theta_{\text{RCH}_2\text{O}^*} + \theta_{\text{RCHOH}^*} + \theta_{\text{RCOH}^*} + \theta_{\text{RCHOOCC}_2\text{H}_5^*} + \theta_{\text{RCH}_2\text{OH}^*} + \theta_{\text{RCOOC}_2\text{H}_5^*} + \theta_{\text{H}_2\text{O}^*} + \theta_* = 1$$